UNIVERSITÀ DEGLI STUDI FIRENZE

Machine Learning in Complex Systems

Duccio Fanelli
Dipartimento di Fisica e Astronomia
Università di Firenze

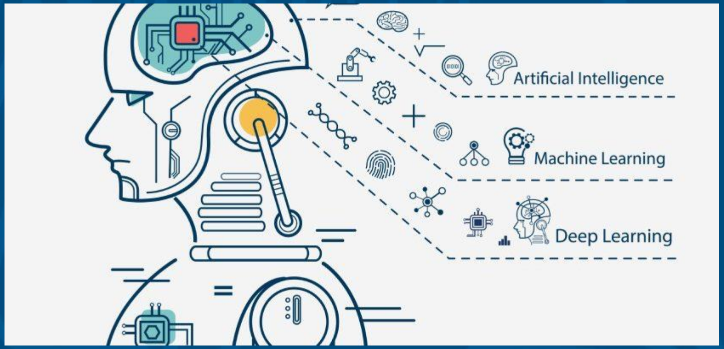

29 gennaio 2025

UNIVERSITÀ DEGLI STUDI FIRENZE

CSDC
CENTRO STUDI DINAMICHE COMPLESSE

Relevant expertise with possible foundational impact

Theory of networks, from ordinary to higher order topologies

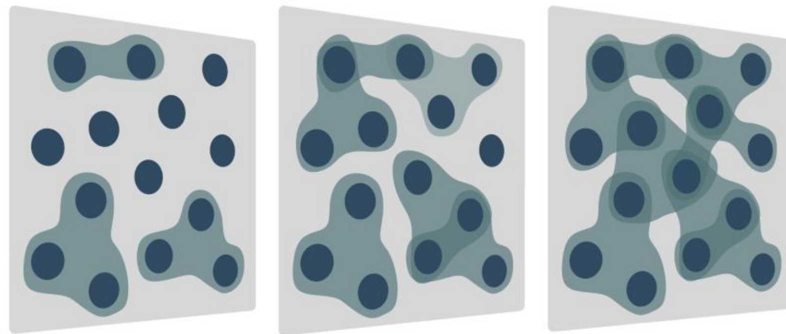

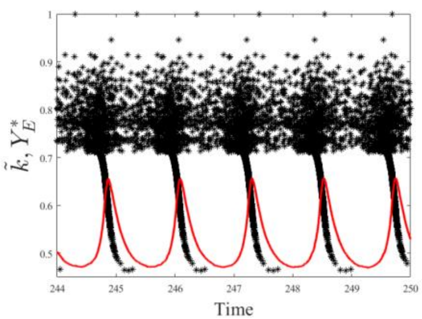

The average fields show ***global activity events***.

Dynamics on networks. Mathematical modeling in neuroscience

Stochastic population dynamics: role of exhogenous/endogenous noise

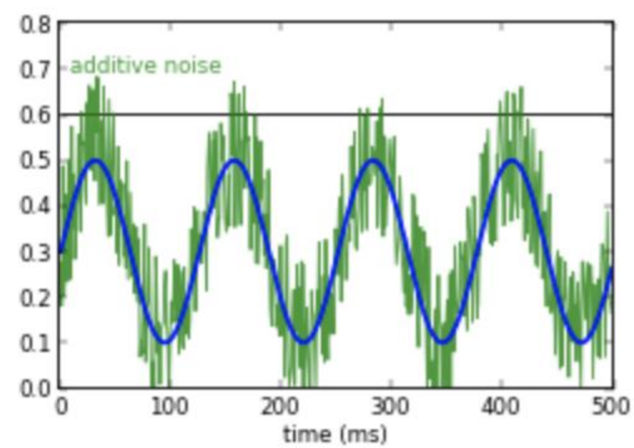

Outline

- **Foundational aspects** of our research (few representative examples):

(a) Spectral approach to learning: pruning and feature detection.

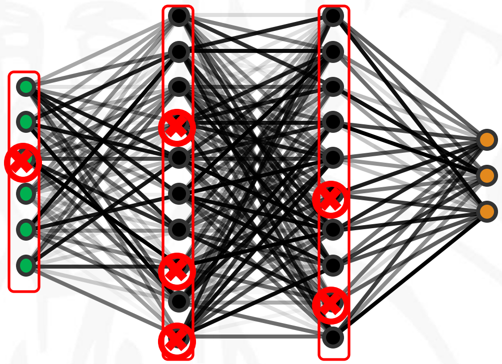

(b) Stochastic Hopfield model: biomimetic classifiers and generative tools

- A list of **selected applications**.

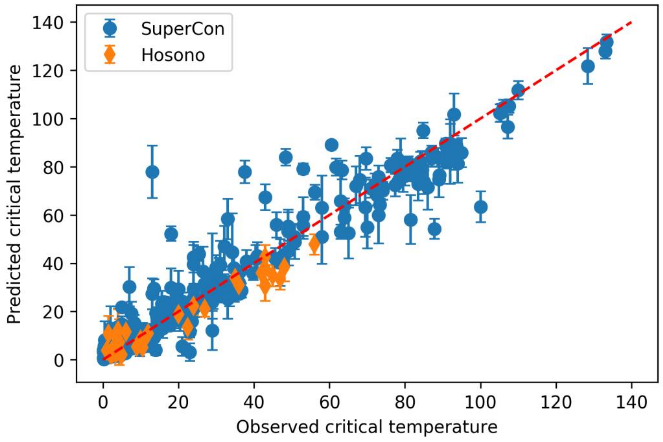

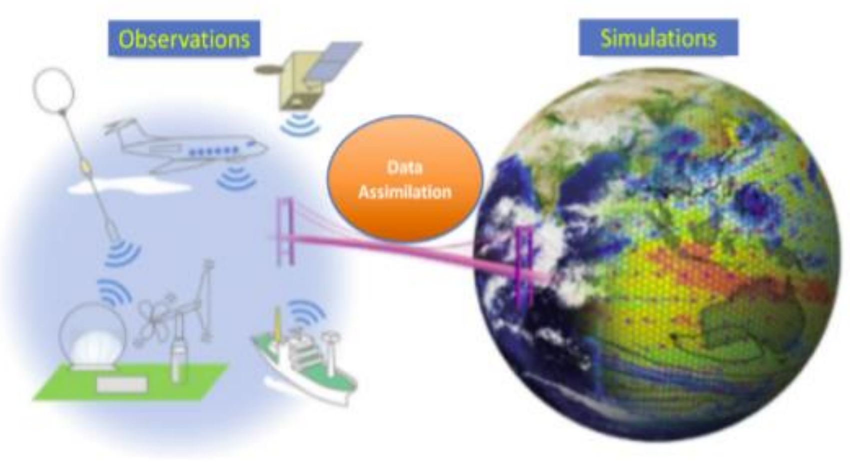

(a). Deep Learning in spectral domain

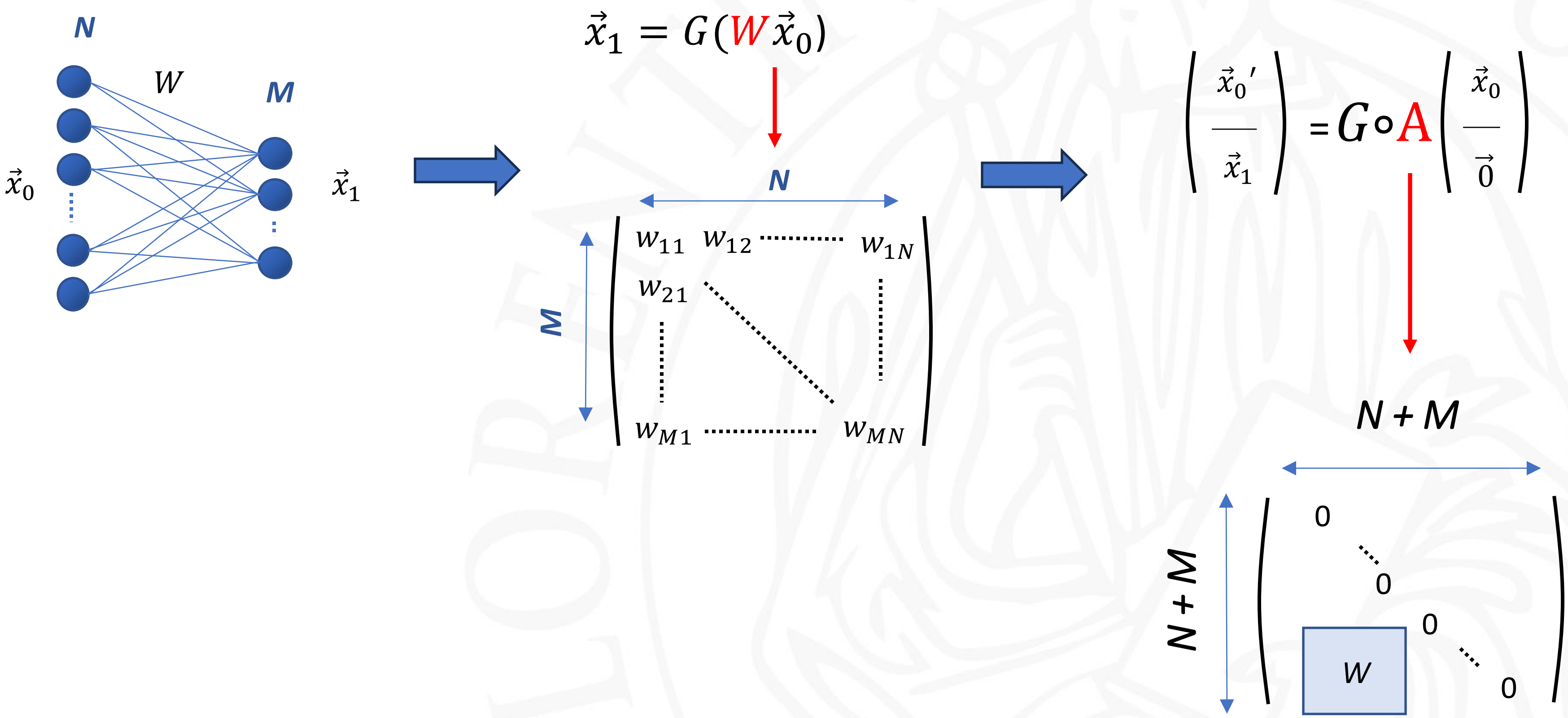

UNIVERSITÀ DEGLI STUDI FIRENZE

(a). Deep Learning in spectral domain

$$\Phi \Lambda \Phi^{-1} = A$$

Spectral Learning

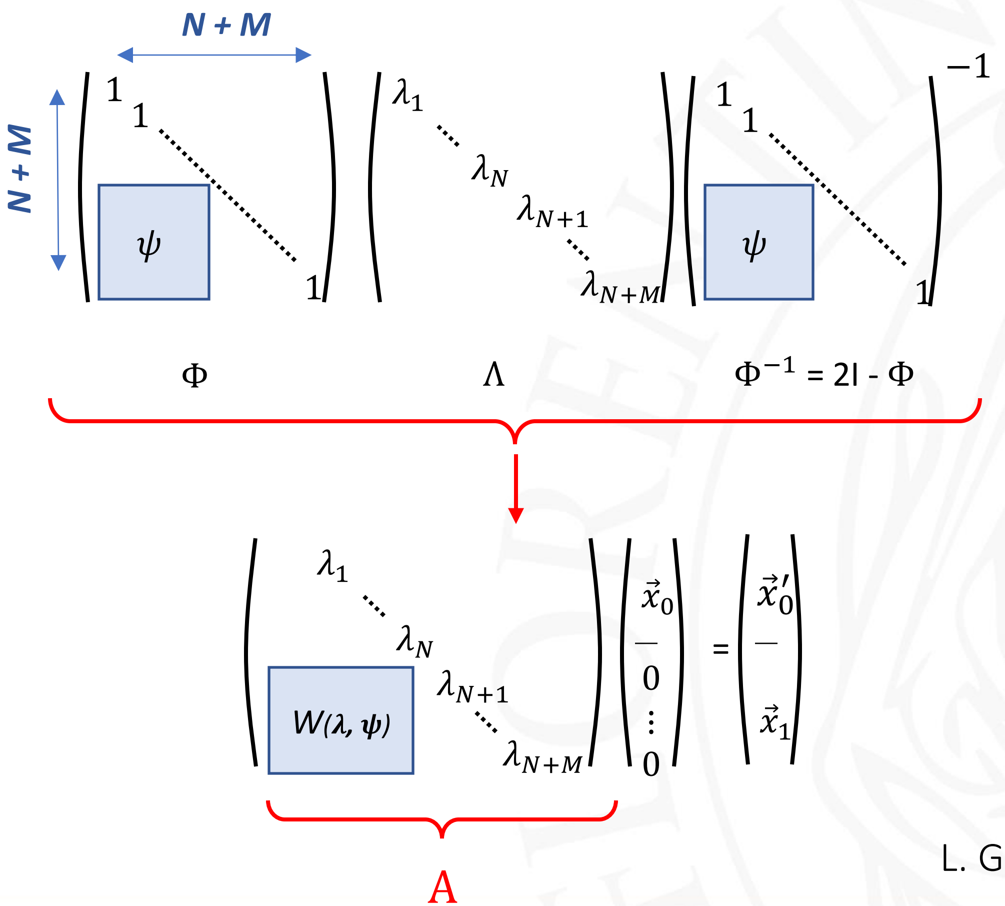

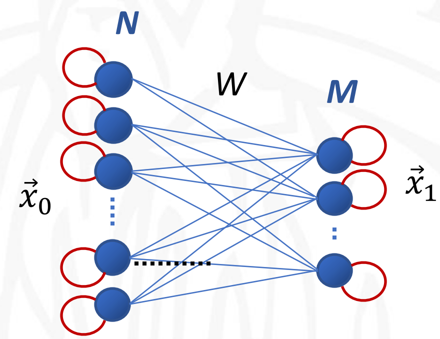

This yields a new set of trainable parameters

L. Giambagli et al. Nat. Commun. 12, 1330 (2021).

$$w_{ij} = \left(\lambda_j^{start} - \lambda_i^{final}\right) \Phi_{ij}$$

- λ_j^{start} modulate the signal on node j
- λ_i^{final} modulate the signal on node i

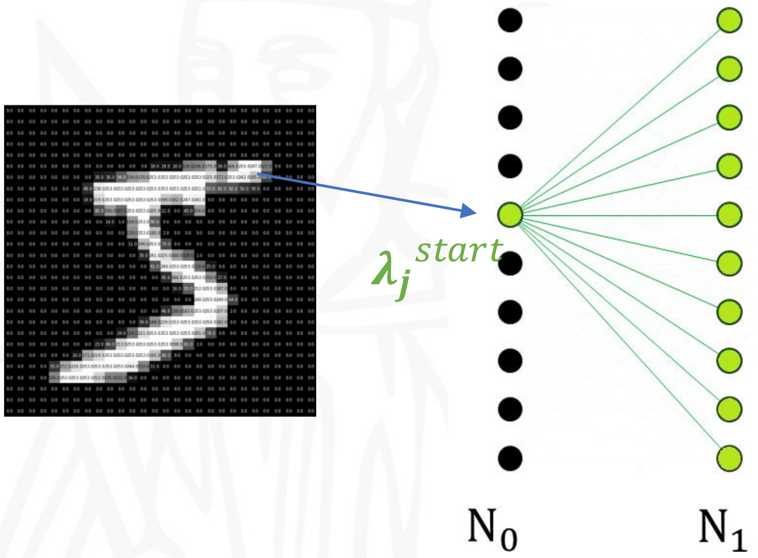

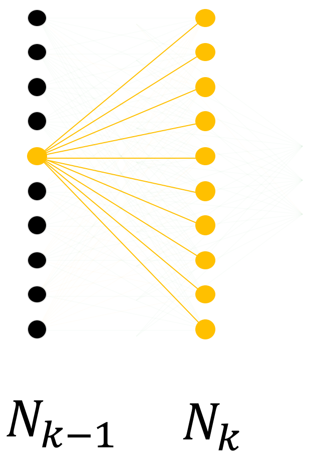

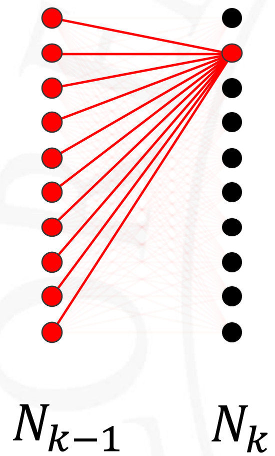

Are the eigenvalues a proxy of the feature relevance?

Buffoni, Giambagli, Chicchi

L. Buffoni, et al. *Scientific reports* 12.1 (2022): 1-9.

Example: the MNIST dataset

A simple real dataset: images of zeros and ones → $\vec{x}_0 \in R^{784}$

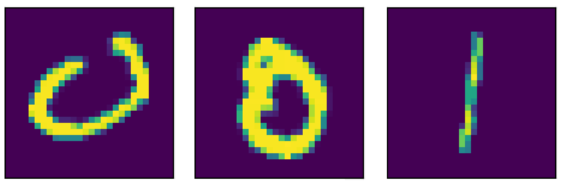

....

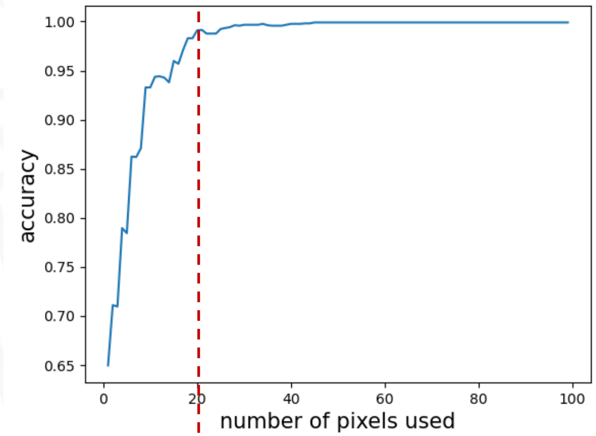

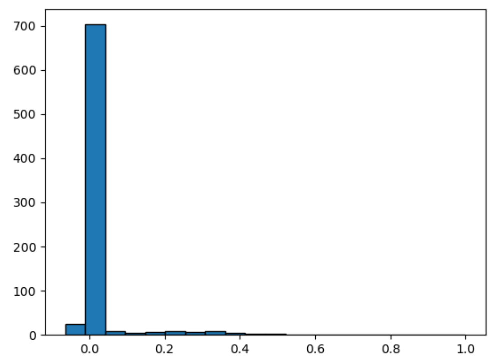

Eigenvalues' distribution

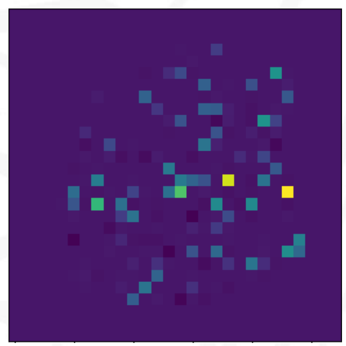

Colormap: eigenvalues

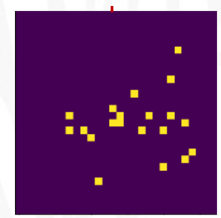

Example: the MNIST dataset

By applying the mask to the input images, we see what the network is looking at:

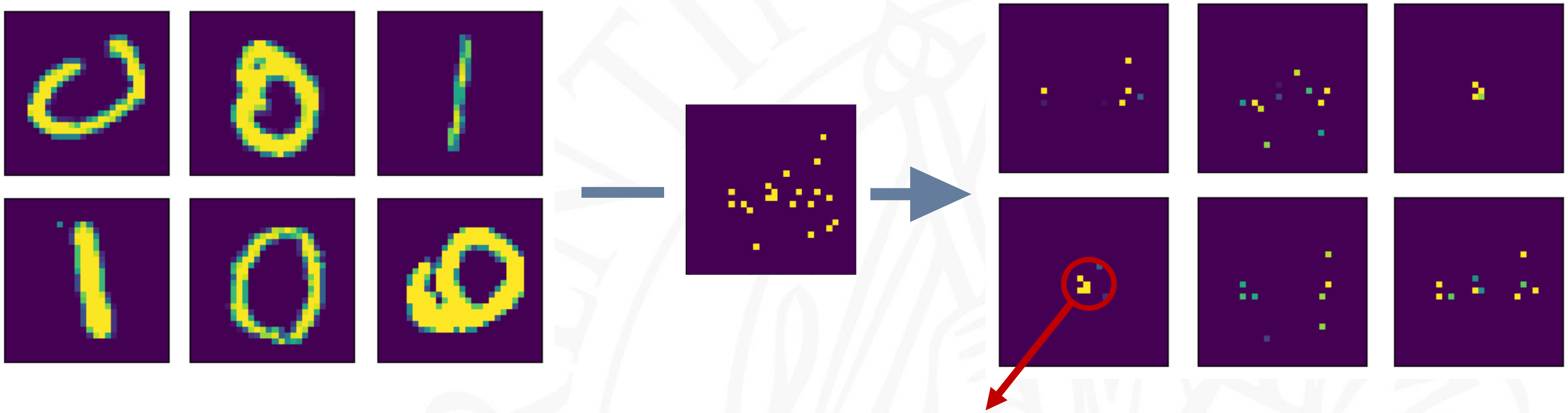

To flag the input as "1", the network checks if the central pixels are turned active

L. Chicchi, et al. arXiv preprint arXiv:2406.01183 (2024)

Chicchi, Febbe

(b). Stochastic Hopfield Model

$$\tau \dot{x}_i(t) = -x_i(t) + \frac{1}{\sqrt{N}} \sum_j A_{ij} f\left(x_j(t)\right) + \sum_j G_{ij}\ \eta_j$$

- x_i stands for the activity on the neuron $\boldsymbol{i}$
- A is the adjacency matrix of the network;
- G defines the covariance matrix of noise.

$$f(x) = \frac{x^2}{c + x^2}$$ Firing rate

A biologically sensible model

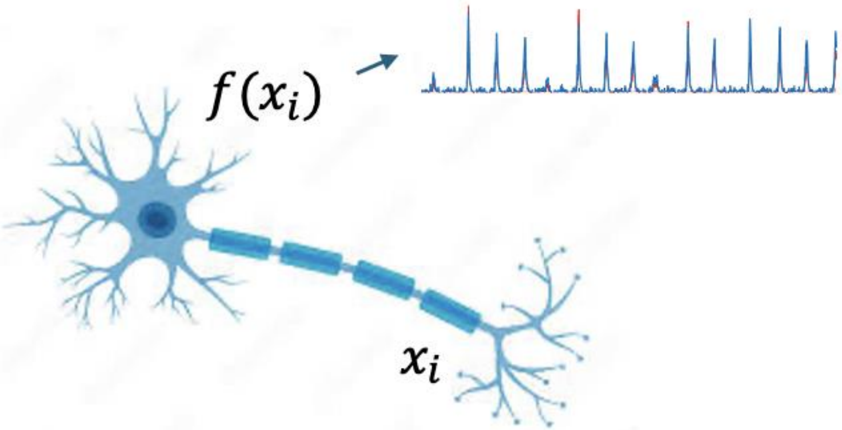

Marino, Raffaele, et al. Machine Learning: Science and Technology 5.3 (2024): 035087;
Chicchi, Lorenzo, et al. arXiv preprint arXiv:2409.13470 (2024).

- Procedure to plant a family of determinist stable attractors
  (hint: make use of the spectral decomposition of A)

- Analytically characterize the stochastic attractors under the linear noise approximation
  (hint: solve associated Fokker-Planck, Langevin eqs. as a function of A and G)

- Train A and G to direct different items towards distinct stochastic attractors
  (hint: backpropagation through time, noise helps to classify)

- Sample the stochastic attractor to generate novel data points

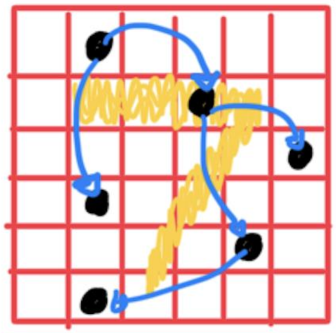

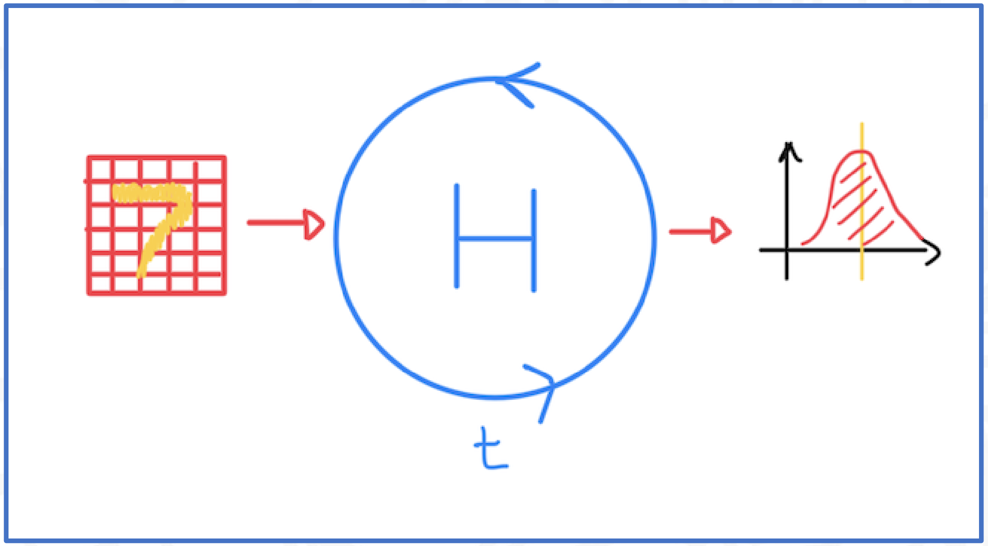

- Procedure to plant a family of determinist stable attractors (hint: make use of the spectral decomposition of A)
- Analytically characterize the stochastic attractors under the linear noise approximation (hint: solve associated Fokker-Planck, Langevin eqs. as a function of A and G)
- Train A and G to direct different items towards distinct stochastic attractors (hint: backpropagation through time, noise help to classify)
- Sample the stochastic attractor to generate novel data points

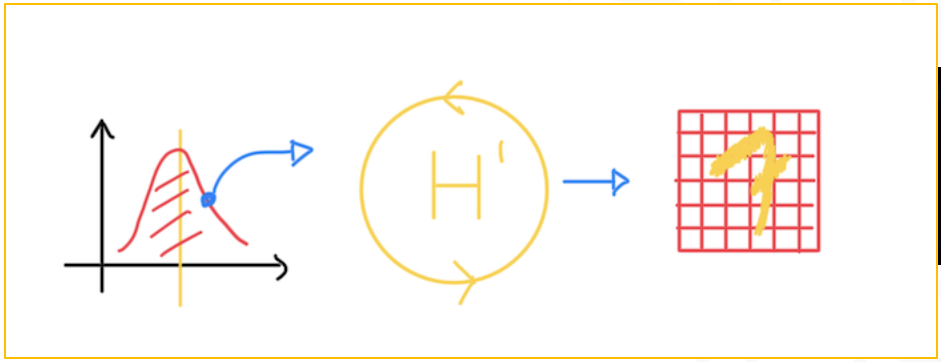

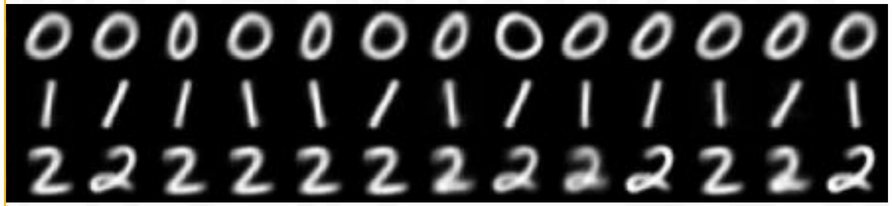

Generated digits

Chicchi, Febbe, Marino, Pacifico

Application 1: Find new supeconductors

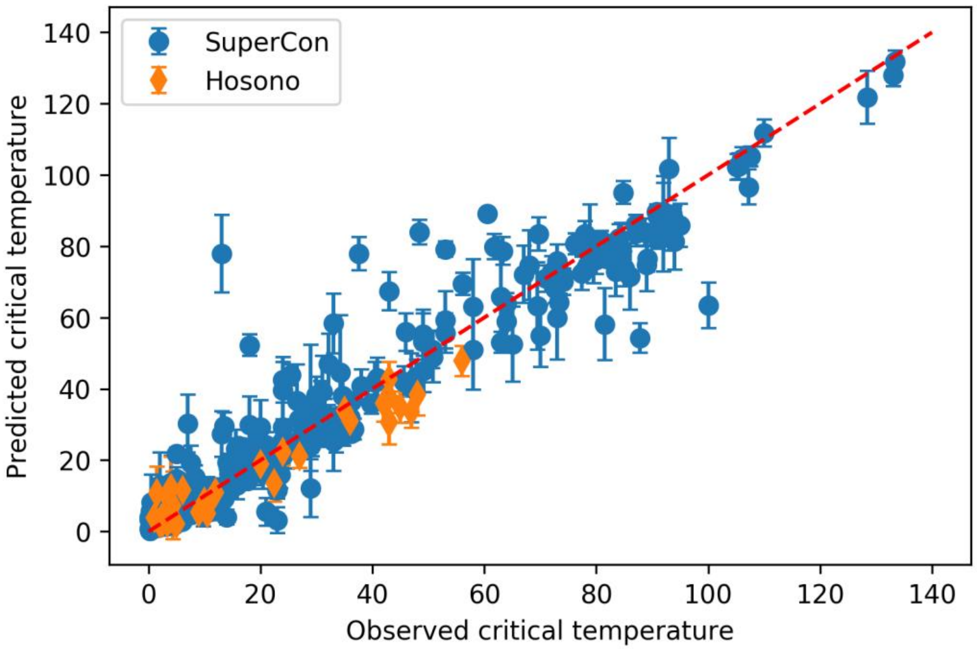

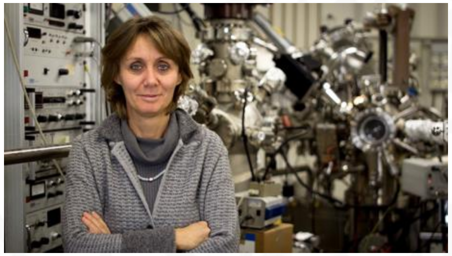

Root mean square error 9.5 K, r^2=0.95 for a latent space of d=300

Predicted vs. **measured critical temperature**, T_c (K). The blue circles refer to materials from the **SuperCon database**. A fraction of 20% of the total is randomly selected as part of the testset, while the remaining 80% is used for training. The operation is repeated 50 times and the collected temperatures from each independent run stored for further processing. The orange diamonds refer to the **39 superconducting materials** present in the Hosono database. This latter contains a total of 207 (superconducting and non-superconducting) compounds.

The experiment

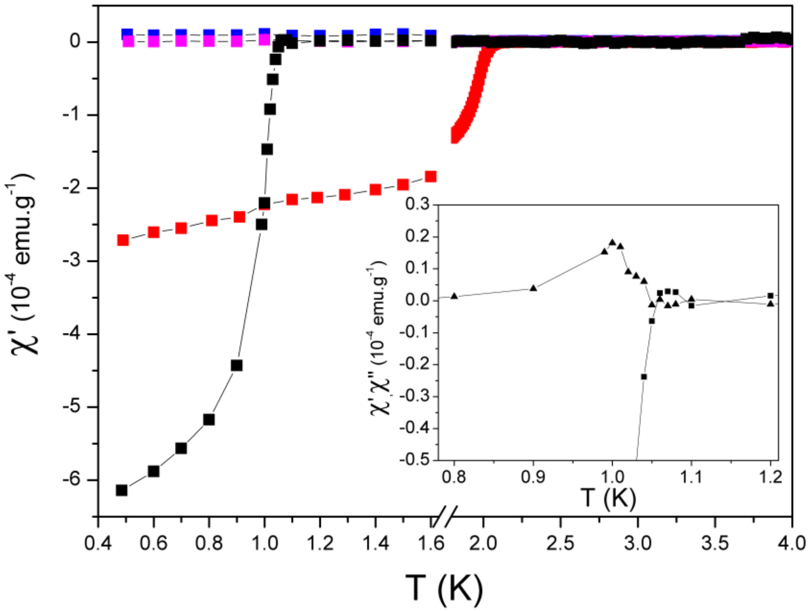

Temperature dependence of the **real part of the susceptibility** measured in zero static field for the four investigated samples: Pd_3HgTe_3 (blue and magenta for sample prepared at 350 and 500 °C, respectively), PdBiTe (red), and Pd_2NiTe_2 (black).

Measurement of a magnetic moment of a sample which is exposed to an oscillating external magnetic field. The detection of a diamagnetic signal that is proportional to the volume fraction is an indication of the presence of a superconducting phase.

Temagamite samples (blue and magenta) do not reveal any sizeable diamagnetic susceptibility, while the clear onset of diamagnetic shielding is visible at ***T*=2.10K** for michenerite (red) and, even more pronounced, at ***T*=1.06 K** for monchetundraite (black).

Predicted critical temperatures by the ML approach:

michenerite: 1.6(0.8) K
monchetundraite: 1.18(0.7) K

C. Pereti, et al. npj Computational Materials 9 71 (2023)

Application 2: volcanic temperature / pressure

UNIVERSITÀ DEGLI STUDI FIRENZE

	Index	T (C)	P (kbar)	CaTiAl2O6	CaTs	Es	CaCrT
1812	Higgins 1	1025	4.85	0.004080996	0.02367	0	
79	52	1060	2.32	0.024016852	0.00654	0.04401	
2001	Neave201	1180	4.3	0.036071859	0.04921	0	
4789	DiFiore21-	1180	0.001	0.033160037	0	0.34304	
751	5216	1300	13	0.008823796	0.1423	0.01241	
2256	Pontesilli_	1100	4	0.036771241	0.10751	0.12066	
2564	Pontesilli_	1100	4	0.038649591	0.12553	0.18479	
2399	Pontesilli_	1100	4	0.040858432	0.09202	0.18201	
6260	DiFiore21-	1150	0.001	0.037280738	0.02608	0.33588	
3302	DiFiore21-	1180	0.001	0.002852696	0	0.31525	
5108	DiFiore21-	1180	0.001	0.03078503	0	0.3721	
3168	Beard_19-	800	2	0.052135745	0	0.28589	
5058	DiFiore21-	1180	0.001	0.030222314	0	0.36843	
2620	Masotta_	1050	4	0.031849776	0.05823	0.11225	
1292	5527	1200	15	0.037671034	0.12379	0	
612	20078	1435	26	0.007217169	0.11337	0.00959	
3458	DiFiore21-	1180	0.001	0.037303557	0.03475	0.32896	
3922	DiFiore21-	1180	0.001	0.033387837	0.0225	0.30545	
4556	DiFiore21-	1180	0.001	0	0	0.28438	0.00
5884	DiFiore21-	1150	0.001	0.025600052	0.01453	0.23361	
5209	DiFiore21-	1180	0.001	0.027693596	0	0.40606	
2068	Pontesilli_	1100	4	0.042769361	0.10728	0.16298	
424	4587	1370	16	0.005327912	0.15512	0.00982	
4306	DiFiore21-	1180	0.001	0.036359704	0.00583	0.35813	
31	3985	1000	2	0.013214101	0.01105	0.02584	
6205	DiFiore21-	1150	0.001	0.034386548	0.00686	0.352	
3012	Hunsen_1	1155	1	0.01773597	0.03708	0.10769	

Database

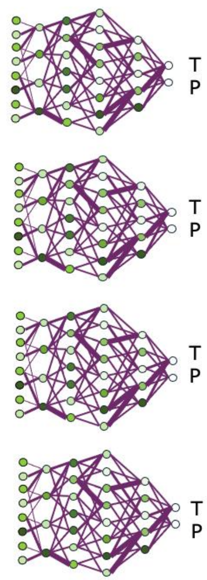

$< T >$
$< P >$
σ_T
σ_P

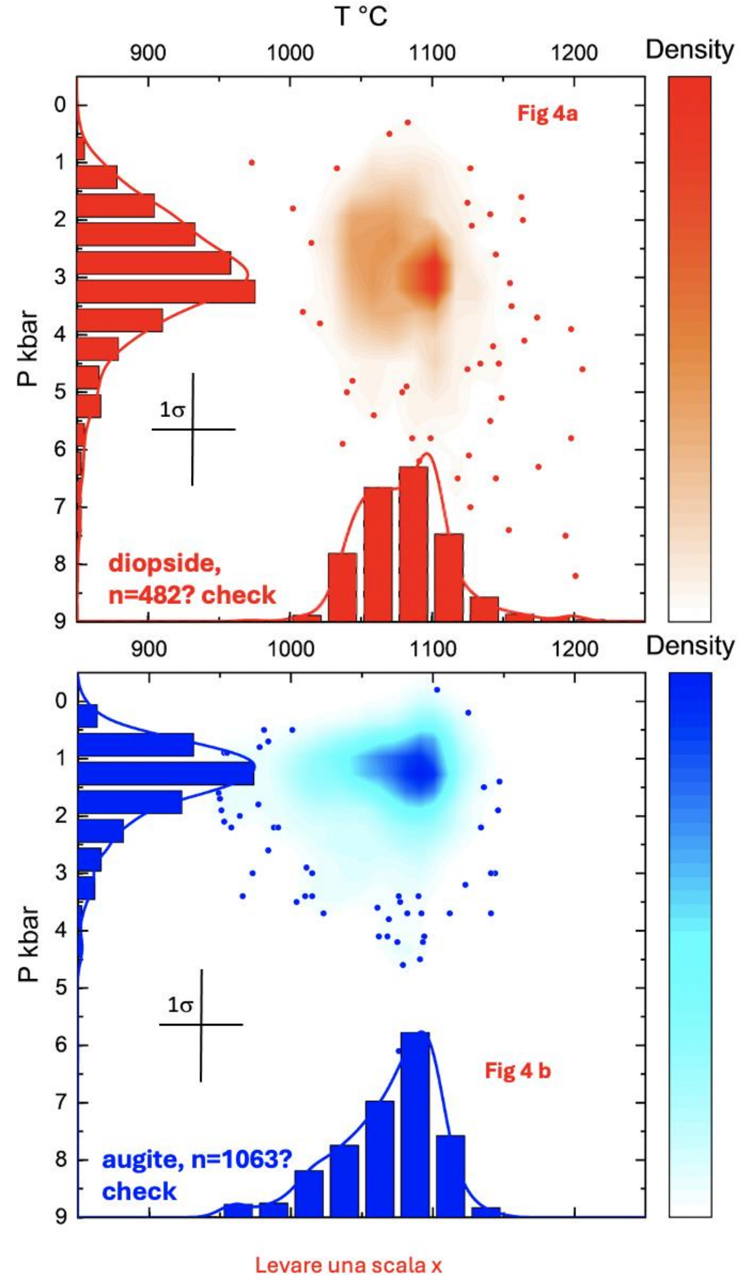

L. Chicchi, et al. Earth and Planetary Science Letters 620 (2023)

Application 3: Integrated spatially resolved whole transcriptomes of single cells

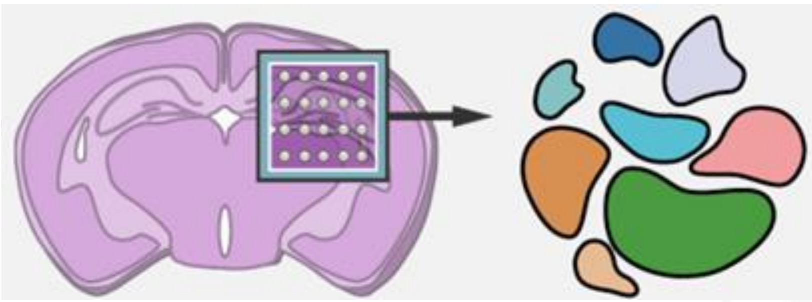

Integration of scRNA-seq data with spatial data

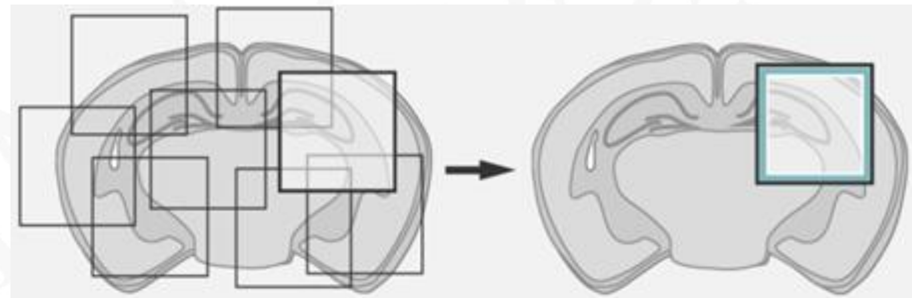

Integration of spatial data with histology

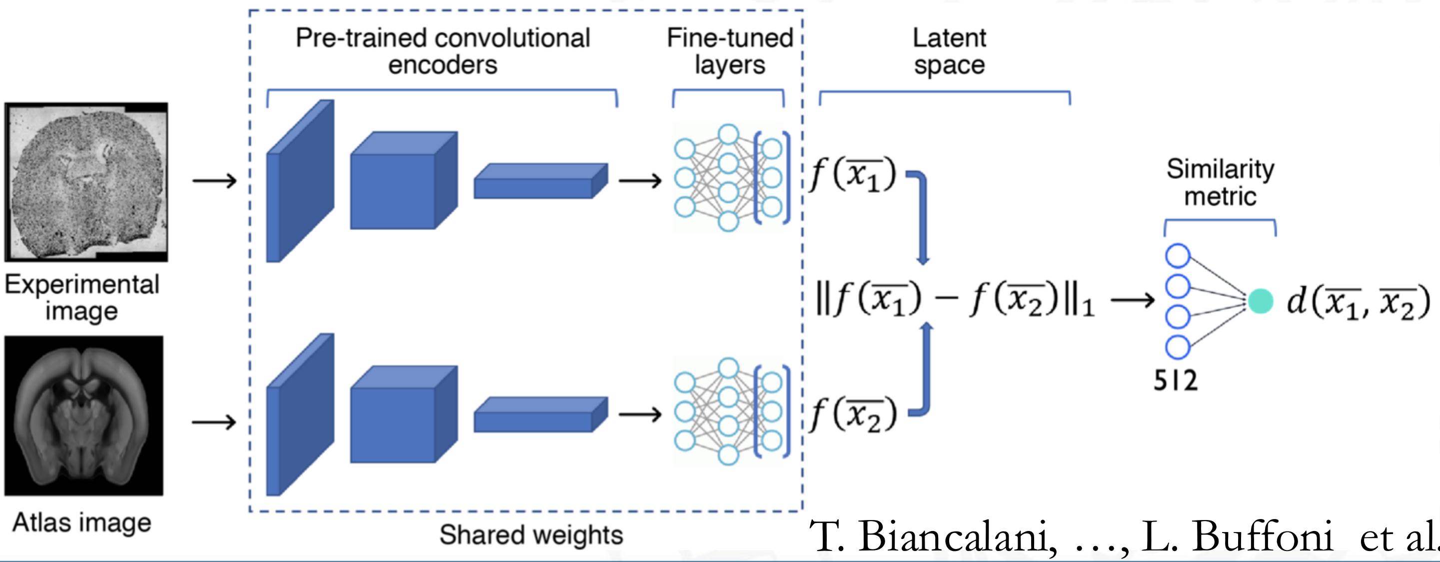

T. Biancalani, …, L. Buffoni et al. Nature Methods (2021)

UNIVERSITÀ DEGLI STUDI FIRENZE

Application 4: time series analysis

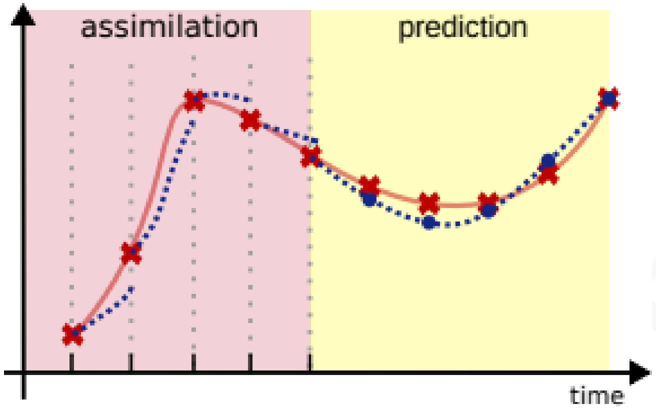

Assimilation and prediction of chaotic system combining model equations and neural network

Forecasting and financial market

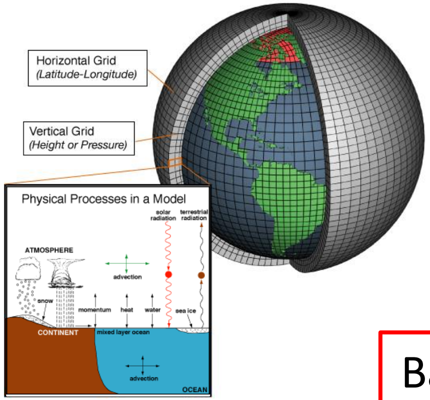

CONSORZIO LaMMA

Bagnoli, Baia

TECNOLINK

Peri